

Disruption of Poly(ADP-ribosyl)ation Mechanisms Alters Responses of Arabidopsis to Biotic Stress^{1[C][W][OA]}

Lori Adams-Phillips², Amy G. Briggs², and Andrew F. Bent*

Department of Plant Pathology (L.A.-P., A.G.B., A.F.B.) and Program in Cellular and Molecular Biology (A.G.B.), University of Wisconsin, Madison, Wisconsin 53706

Poly(ADP-ribosyl)ation is a posttranslational protein modification in which ADP-ribose (ADP-Rib) units derived from NAD⁺ are attached to proteins by poly(ADP-Rib) polymerase (PARP) enzymes. ADP-Rib groups are removed from these polymer chains by the enzyme poly(ADP-Rib) glycohydrolase (PARG). In animals, poly(ADP-ribosyl)ation is associated with DNA damage responses and programmed cell death. Previously, we hypothesized a role for poly(ADP-ribosyl)ation in plant defense responses when we detected defense-associated expression of the poly(ADP-ribosyl)ation-related genes *PARG2* and *NUDT7* and observed altered callose deposition in the presence of a chemical PARP inhibitor. The role of poly(ADP-ribosyl)ation in plant defenses was more extensively investigated in this study, using Arabidopsis (*Arabidopsis thaliana*). Pharmacological inhibition of PARP using 3-aminobenzamide perturbs certain innate immune responses to microbe-associated molecular patterns (flg22 and elf18), including callose deposition, lignin deposition, pigment accumulation, and phenylalanine ammonia lyase activity, but does not disrupt other responses, such as the initial oxidative burst and expression of some early defense-associated genes. Mutant *parg1* seedlings exhibit exaggerated seedling growth inhibition and pigment accumulation in response to elf18 and are hypersensitive to the DNA-damaging agent mitomycin C. Both *parg1* and *parg2* knockout plants show accelerated onset of disease symptoms when infected with *Botrytis cinerea*. Cellular levels of ADP-Rib polymer increase after infection with avirulent *Pseudomonas syringae* pv *tomato* DC3000 *avrRpt2*⁺, and pathogen-dependent changes in the poly(ADP-ribosyl)ation of discrete proteins were also observed. We conclude that poly(ADP-ribosyl)ation is a functional component in plant responses to biotic stress.

Current models for the overall organization of plant immune systems include preformed defenses and infection-induced basal and *R* gene-mediated defenses (Jones and Dangl, 2006; Bent and Mackey, 2007; McDowell and Simon, 2008). Basal immune responses are mediated by receptors that recognize ubiquitously expressed, highly conserved microbe-associated molecular patterns (MAMPs) such as bacterial flagellin or EF-Tu proteins or fungal chitin. Many pathogens express effector proteins that suppress basal host immune responses, but *R* gene-mediated defenses can be activated when host *R* proteins recognize the presence

or activity of specific pathogen effectors (also called avirulence [*avr*] proteins). *R* gene activation usually induces a rapid, multifactor defense, including a programmed cell death response known as the hypersensitive response. Both basal and *R* gene-mediated defenses can engage protein phosphorylation, ion fluxes, reactive oxygen species (ROS) production, and production of defense signaling compounds such as salicylic acid (SA), nitric oxide, ethylene, and jasmonic acid (Feys and Parker, 2000; Hammond-Kosack and Parker, 2003). These signals, among other things, induce the expression of defense-associated genes and microRNAs that promote antimicrobial functions and protect the cell from its own defense systems.

One prominent cellular response to pathogen infection is cell wall reinforcement, which can prevent further ingress of the pathogen and also restrict the passage of nutrients and water (Grant and Mansfield, 1999; Lee et al., 2001). Cell wall reinforcement in response to pathogens includes the formation of cell wall appositions, or papillae, containing Hyp-rich glycoproteins, phenylpropanoid compounds such as monolignols, and callose (Bestwick et al., 1995, 1997; Soylyu et al., 2005; Underwood and Somerville, 2008). Hydrogen peroxide and other ROS, often derived from NADPH oxidase complexes and/or peroxidase activity at sites of papilla formation, contribute to cross-linking of proteins and phenolics at the cell wall, resulting in a structurally reinforced cell wall (Bestwick

¹ This work was supported by the U.S. Department of Agriculture National Research Initiative (grant no. 2006-35319-17214 to A.F.B.), the U.S. Department of Energy Office of Basic Energy Sciences (grant no. DE-FG02-02ER15342 to A.F.B.), and a Ruth L. Kirschstein National Research Service Award from the National Institutes of Health (grant no. 5F32GM075599-02 to L.A.-P.).

² These authors contributed equally to the article.

* Corresponding author; e-mail afbent@wisc.edu.

The author responsible for distribution of materials integral to the findings presented in this article in accordance with the policy described in the Instructions for Authors (www.plantphysiol.org) is: Andrew F. Bent (afbent@wisc.edu).

[C] Some figures in this article are displayed in color online but in black and white in the print edition.

[W] The online version of this article contains Web-only data.

[OA] Open Access articles can be viewed online without a subscription.

www.plantphysiol.org/cgi/doi/10.1104/pp.109.148049

et al., 1997; Thordal-Christensen et al., 1997; Brown et al., 1998; Soyly et al., 2005). Some bacterial and oomycete effectors suppress callose deposition as a virulence mechanism (Hauck et al., 2003; DebRoy et al., 2004; de Torres et al., 2006; Sohn et al., 2007).

Previously, we found a poly(ADP-Rib) glycohydrolase (*PARG2*) and a Nudix hydrolase active on ADP-Rib and NADH (*NUDT7*) among a small group of less than 40 genes significantly up-regulated in multiple *R/avr* interactions between *Arabidopsis thaliana* and *Pseudomonas syringae* pv *tomato* DC3000 (*Pst* DC3000; Adams-Phillips et al., 2008). *nudt7* plants were more resistant to virulent and avirulent *Pst* DC3000 (Bartsch et al., 2006; Jambunathan and Mahalingam, 2006; Ge et al., 2007; Adams-Phillips et al., 2008) and also displayed a greatly reduced hypersensitive response to avirulent *Pst* DC3000 (Adams-Phillips et al., 2008). We also found that pharmacological inhibition of poly(ADP-Rib) polymerase (PARP) blocked the formation of callose-containing cell wall depositions induced by the MAMPs flg22 and elf18 (Adams-Phillips et al., 2008). This suggested a role for poly(ADP-ribosyl)ation in the pathways that regulate pathogen-elicited callose deposition and plant innate immune responses.

Poly(ADP-ribosyl)ation is an important posttranslational modification in many eukaryotes (Otto et al., 2005; Hassa and Hottiger, 2008). It is biochemically and functionally distinct from mono-ADP-ribosylation. At the organismal level, poly(ADP-ribosyl)ation in animals contributes to the pathology of stroke, ischemia, heart attack, and chemotherapy (Jagtap and Szabo, 2005). Poly(ADP-ribosyl)ation is carried out by PARPs, which use NAD⁺ as a substrate to catalyze both the attachment and elongation of ADP-Rib polymers on acceptor proteins. Automodified PARP and other poly(ADP-ribosyl)ated nuclear proteins (Huletsky et al., 1989) can affect chromatin structure, transcription, replication, and DNA repair processes through PARP-mediated recruitment of other proteins (Masson et al., 1998; Simbulan-Rosenthal et al., 1999; Ahel et al., 2009). Therefore, PARP can act as a DNA damage sensor (Petrucco, 2003; Schreiber et al., 2006; Roldan-Arjona and Ariza, 2009). In addition, PARP and poly(ADP-ribosyl)ation can regulate cellular processes by modulating cellular levels of NAD⁺. Strong PARP activation can cause massive consumption of NAD⁺, which can alter cellular reduction/oxidation states, impact nicotinamide levels, and induce ATP depletion (Hashida et al., 2009).

Eukaryotic organisms (excluding yeast) express multiple PARP proteins, all bearing a conserved C-terminal PARP catalytic domain. The *Arabidopsis* genome encodes at least three putative PARPs (Hunt et al., 2004; Otto et al., 2005). Use of pharmacological PARP inhibitors is a common way of overcoming such potential functional redundancy and also allows conditional inactivation of PARP activity. 3-Aminobenzamide (3AB) is a widely used PARP inhibitor in both animal (Bryant et al., 2005; Beauchamp et al., 2009; Ding et al.,

2009; Hernandez et al., 2009) and plant (Phillips and Hawkins, 1985; Berglund et al., 1996; Amor et al., 1998; Tian et al., 2000; Adams-Phillips et al., 2008; Ishikawa et al., 2009) studies and has been shown to inhibit plant PARP enzymatic activity (Chen et al., 1994; Babiychuk et al., 1998). 3AB has also been used to demonstrate the linkage between PARP and PARG activity in plants. For example, application of 3AB restored wild-type levels of ADP-Rib polymer in *Arabidopsis parg1* (*tej*) mutant plants that otherwise accumulate 5-fold higher levels of poly(ADP)-Rib than wild-type seedlings (Panda et al., 2002).

PARG hydrolyzes the ADP-Rib polymers synthesized by PARP (Davidovic et al., 2001). As such, PARG is often thought to reverse, or counteract, PARP activity. PARG does not, however, restore the large amounts of NAD⁺ that can be consumed through PARP activity, and PARG's activity can increase cellular pools of free ADP-Rib, a known cell death signal in mammalian cells (Andrabi et al., 2006). Hence, PARG can either counteract or further contribute to the impacts of PARP activation, depending on cellular context. Known animal genomes encode a single *PARG* gene (Ame et al., 1999), and mutation of *PARG* leads to the accumulation of toxic ADP-Rib polymers and is lethal in mice and *Drosophila* (Hanai et al., 2004; Koh et al., 2004). *Arabidopsis* is a rare example of a eukaryote with two *PARG* genes, which are present due to a gene duplication (At2g31865 and At2g31870). Much less is known about the functional role of PARG in plants, but it has been shown that PARG1 plays a role in regulating circadian rhythms in *Arabidopsis* (Panda et al., 2002).

Free ADP-Rib (which is generated by PARG) is rapidly degraded to AMP by certain nudix hydrolase (*NUDT*) enzymes, including *Arabidopsis* *NUDT2* and *NUDT7* (Ogawa et al., 2005). ADP-Rib-specific nudix hydrolases are thought to have multiple roles: they (1) reduce the high levels of toxic free ADP-Rib, (2) reestablish energy levels by supplying a source for ATP, and (3) contribute to NAD⁺ maintenance (Rossi et al., 2002; Ogawa et al., 2005, 2009; Ishikawa et al., 2009). As noted above, multiple groups have identified impacts of *Arabidopsis nudt7* mutants on responses to pathogen (Bartsch et al., 2006; Jambunathan and Mahalingam, 2006; Ge et al., 2007; Adams-Phillips et al., 2008).

There is evidence that plant PARPs are structurally and functionally homologous to mammalian PARP proteins (Chen et al., 1994; O'Farrell, 1995; Babiychuk et al., 1998; Doucet-Chabeaud et al., 2001). DNA damage induced by ionizing radiation activates *Arabidopsis* *PARP1* and *PARP2* gene expression (Doucet-Chabeaud et al., 2001). Application of 3-methoxybenzamide, a chemical PARP inhibitor, alters rates of homologous recombination in *Arabidopsis* and tobacco (*Nicotiana tabacum*) plants (Puchta et al., 1995), further suggesting a role for poly(ADP-ribosyl)ation in DNA repair in plants. Accumulating evidence suggests that poly(ADP-ribosyl)ation is an important part of the plant

response to abiotic stress (De Block et al., 2005; Vanderauwera et al., 2007). For example, *parp1/parp2* double knockdown Arabidopsis plants display increased resistance to drought, high light, and oxidative stresses (De Block et al., 2005), and PARP inhibitors such as 3AB protect soybean (*Glycine max*) and tobacco cell suspensions from oxidative and heat shock-induced programmed cell death (Amor et al., 1998; Tian et al., 2000). 3AB was also shown to inhibit oxidative stress-induced Phe ammonia lyase (PAL) activity in *Catharanthus roseus* tissue culture (Berglund et al., 1996).

Given the demonstrated roles of PARP in plant abiotic stress responses (De Block et al., 2005; Vanderauwera et al., 2007) and in animal cell stress and cell death (Heeres and Hergenrother, 2007; David et al., 2009), poly(ADP-ribosyl)ation has received surprisingly little research attention regarding plant immunity and biotic stress responses. In this study, we used a combination of PARP inhibitors, genetic mutant analysis, and biochemical assays to further dissect the role of poly(ADP-ribosyl)ation in plant-pathogen interactions. We determined that although PARP inhibition and *PARG* gene disruption do not disrupt initial responses such as ROS production, they impact several MAMP-triggered responses downstream of ROS production, including callose and lignin deposition and phenylpropanoid pathway activation, and can accelerate the onset of the symptoms caused by the necrotrophic pathogen *Botrytis cinerea*. We also detected changes in the abundance of ADP-Rib polymers and poly(ADP-ribosyl)ated proteins during various Arabidopsis-pathogen interactions. These data provide further evidence that poly(ADP-ribosyl)ation plays significant, diverse roles in the coordination of plant responses to biotic stress.

RESULTS

PARP Inhibitor Impacts MAMP-Induced Plant Responses Downstream of ROS Production

Our previous study revealed that pharmacological inhibition of PARP blocks callose-containing cell wall depositions induced by either flg22 or elf18 in Arabidopsis (Adams-Phillips et al., 2008). As a follow-up to these experiments, we examined the effects of PARP inhibitor on other instances of induced callose production. We discovered that treatment with the PARP inhibitor 3AB does not block wound-induced callose deposition, nor does it reduce the constitutively active callose observed in *mekk1*⁻ mutants (Suarez-Rodriguez et al., 2007; Fig. 1A), indicating that 3AB specifically blocks MAMP-induced callose deposition. It is also unlikely that PARP inhibitor directly impacts the PMR4 callose synthase enzyme that is responsible for most MAMP- and wound-induced callose synthesis (Jacobs et al., 2003; Nishimura et al., 2003; Kim et al., 2005; Soylyu et al., 2005), as no alteration to wound-

induced callose was observed when 3AB was added (Fig. 1A). In general, we found that a higher dose of 3AB was required to block elf18-induced callose deposition than for flg22-induced callose deposition (Supplemental Fig. S1).

To investigate where in the pathway of basal immune signaling 3AB might be acting to disrupt callose deposition, we examined the impact of PARP inhibition on MAMP-elicited production of ROS and induction of two MAMP-induced genes, *WRKY29* and *FRK1*, that are normally expressed within 30 min of MAMP treatment (Asai et al., 2002). We found that flg22- or elf18-induced ROS production and *WRKY29* and *FRK1* gene expression were not significantly altered by 3AB treatment (Fig. 1, B and C). We also observed that 3AB can inhibit callose production when seedlings are treated with PARP inhibitor at 5 h, but not at 24 h, after elicitation with MAMPs (Fig. 1D), supporting the hypothesis that the blockage of callose deposition by PARP inhibitor is independent of early MAMP responses such as ROS production and induction of *WRKY29* and *FRK1* gene expression.

Callose Deposition Blocked by PARP Inhibitor Treatment Can Be Rescued by SA

We further investigated how 3AB may be acting to block elf18- and flg22-induced callose production, as relatively little is known about the pathways that lead to MAMP-induced callose deposition. Clay et al. (2009) recently demonstrated that flg22-induced callose requires induction of multiple pathways, including an ethylene/MYB51-dependent indole-3-glucosinolate biosynthesis pathway and a CYP81F2-dependent pathway. Therefore, we tested the impact of PARP inhibition on additional aspects of the MAMP-induced callose pathway. PARP inhibition by 3AB treatment did not alter flg22-induced *MYB51* or *CYP81F2* gene expression (Fig. 2A). These results suggest that 3AB blockage of MAMP-induced callose may be independent of and/or downstream of the MYB51/ethylene-dependent and CYP81F2/I3G pathways. It has been reported that defects in defense-associated callose deposition in *pen2*, *pcs1*, and *vtc1* mutants can be rescued by SA treatment (Clay et al., 2009). We found that, although treatment of seedlings with only SA or benzothiadiazole (BTH; a chemical analog of SA) does not induce callose deposition, addition of SA or BTH to flg22-treated seedlings can rescue 3AB blockage of flg22-induced callose deposition (Fig. 2B). Furthermore, use of an *npr1* mutant revealed that this rescue by SA of 3AB blockage of callose is independent of *NPR1* (Table I). These results could suggest that PARP inhibition interferes with a SA-dependent, *NPR1*-independent callose pathway upstream of SA biosynthesis or, alternatively, that in the presence of flg22, exogenous application of SA or BTH can activate an independent pathway and bypass the flg22-induced callose deposition pathway that is blocked by PARP inhibition. Callose deposition was still elicited by flg22 treatment in

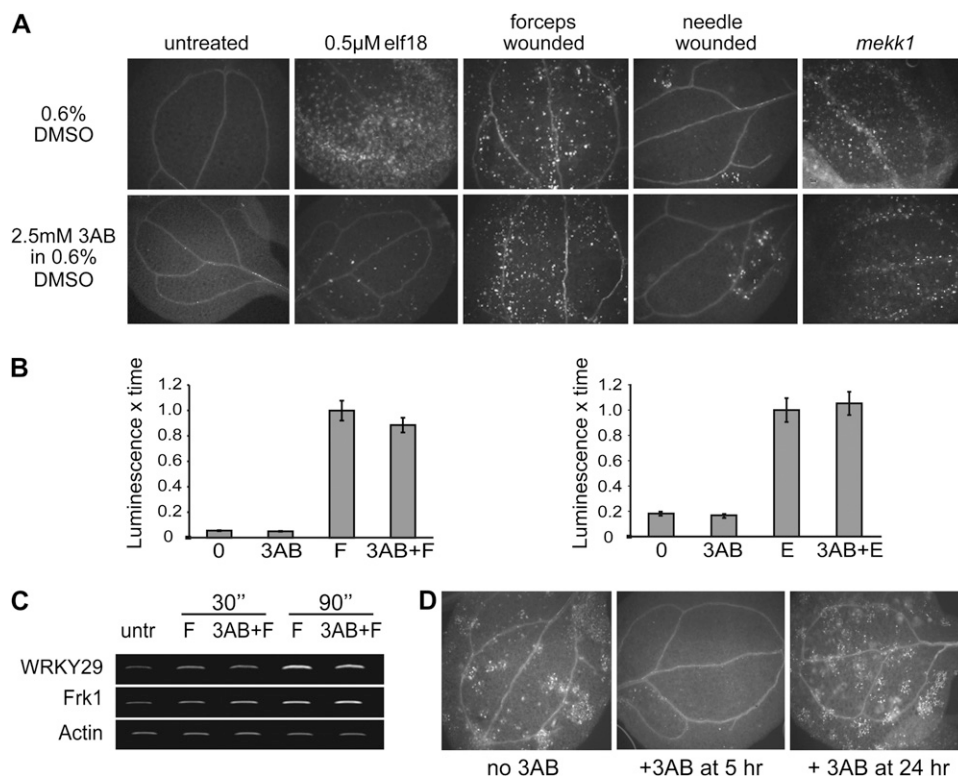


Figure 1. PARP inhibitor 3AB blocks MAMP-induced callose but not wound- or *mekk1*-associated callose; PARP inhibitor also does not block MAMP-induced ROS or gene expression responses. **A**, Callose deposition in 10-d-old *Arabidopsis* seedlings 24 h after the indicated treatment, except *mekk1* mutants were germinated in 3AB and visualized for callose 1 week later. Five-day-old *mekk1* seedlings treated with 3AB for 24 h also produce callose (data not shown). **B**, ROS production in *Arabidopsis* leaf discs that were treated with 3AB 30 min prior to exposure to 1 μ M flg22 (F, left graph) or 1 μ M elf18 (E, right graph). ROS production was measured for 30 min immediately after MAMP exposure, using a luminol-based assay, and area under the curve is presented, normalized to the average area for MAMP-treated samples from the same experiment (means \pm SE are shown for 36 samples from three biological replicates). **C**, MAMP-induced gene expression, as monitored by semiquantitative RT-PCR for *Arabidopsis* seedlings treated with or without 2.5 μ M flg22 and PARP inhibitor for the indicated time intervals. Similar results were obtained in two biological replicates. untr, Untreated. **D**, Callose deposition in *Arabidopsis* seedlings 24.1 h after exposure to 1.0 μ M flg22. Some seedlings were also treated with 2.5 mM 3AB at 5 or 24 h after exposure to flg22. Experiment was repeated twice with similar results.

nahG⁺ (salicylate-degrading) and *sid2*⁻ (salicylate biosynthesis-defective) plants that have greatly reduced SA production (Table I), as was also observed by Clay et al. (2009), which suggests that SA is not required for flg22-induced callose deposition. The above results further define the complex regulatory network that controls pathogen-responsive callose deposition (see "Discussion").

PARP Inhibitor Disrupts Aspects of the Phenylpropanoid Pathway

In addition to our experiments with callose deposition, we examined the effects of PARP inhibitor on lignin deposition, a very different type of pathogen-induced cell wall reinforcement. Lignin is polymerized from soluble phenolics that, along with callose, can be found in pathogen-induced papillae (Lawton and Lamb, 1987; Nicholson and Hammerschmidt,

1992; Bhuiyan et al., 2009). We found that treatment with 3AB reduced elf18-induced guaiacyl lignin accumulation (Fig. 3A). Blockage of elf18-induced guaiacyl lignin is independent of the ability to induce callose deposition; *pnr4* mutants, which are deficient in MAMP-induced callose deposition (Kim et al., 2005), still produce MAMP-elicited lignin (Fig. 3B).

Throughout the course of our experiments with elf18-treated seedlings, we observed that treatment with elf18 peptide elicits the accumulation of a dark brown pigment in the cotyledons of seedlings after several days of growth in liquid medium (Fig. 3C). Treatment of seedlings with *L*- α -aminoxy- β -phenylpropionic acid (AOPP), a chemical inhibitor of PAL activity (Kudakasseril and Minocha, 1986; Prats et al., 2007; Pan et al., 2008), reduces the accumulation of this pigment (Fig. 3D), suggesting that this pigment is likely a product of the phenylpropanoid pathway. In further support of this, seedlings with a mutation in

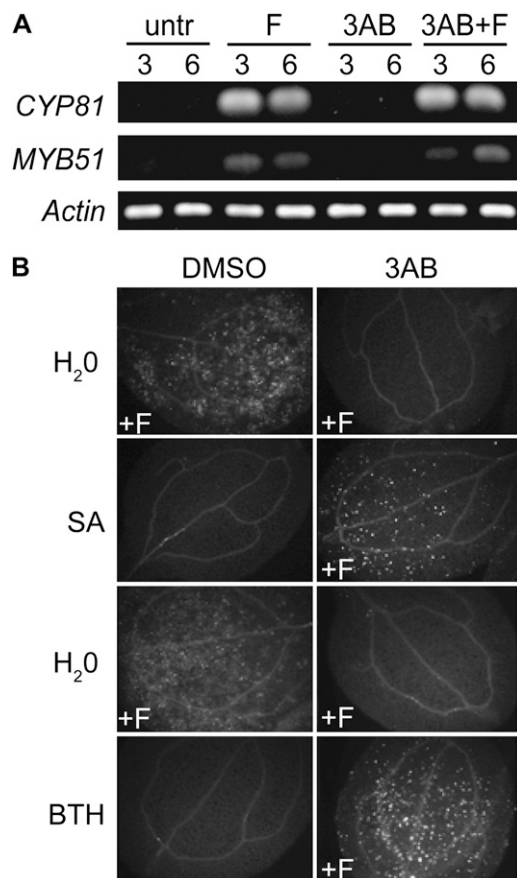


Figure 2. Disruption of callose deposition by PARP inhibitor 3AB is not correlated with *MYB51* or *CYP81F2* mRNA expression and can be rescued by exogenous SA. A, Semiquantitative RT-PCR for Arabidopsis seedlings treated for 3 or 6 h with or without 2.5 μ M flg22 (F) or 2.5 mM 3AB, as indicated. Untr, Untreated. B, Callose deposition in 10-d-old Arabidopsis seedlings treated with distilled, deionized water (H₂O), 1.0 mM SA, or 0.3 mM BTH at 30 min prior to treatment with 0.6% DMSO carrier or 2.5 mM 3AB. Seedlings were then treated with 1 μ M flg22 or distilled, deionized water at 30 min after application of DMSO or 3AB and were fixed 24 h after flg22 elicitation and visualized for callose deposition. Twelve cotyledons per experiment were examined in three independent experiments with similar results, and representative leaves are shown.

the chalcone synthase gene, a key regulator in the production of pigments from the phenylpropanoid pathway, did not accumulate this pigment (data not shown). Interestingly, treatment with PARP inhibitor can block this pigment from accumulating in wild-type seedlings (Fig. 3D), indicating that 3AB may act to inhibit elf18-induced activation of the phenylpropanoid pathway, resulting in reduced pigment and lignin formation. Treatment of seedlings with 3AB significantly reduced PAL activity in elf18-elicited seedlings (Fig. 3E), supporting the Berglund et al. (1996) result that 3AB inhibits PAL activity in *C. roseus* tissue culture protein extracts in response to oxidative stress. Together with the blocked callose deposition, these results indicate that poly(ADP-ribosyl)ation processes

engaged during plant defense may contribute to the regulation of multiple components deposited in pathogen-elicited plant cell wall modifications.

Disruption of PARG1 Gene Expression Exacerbates a Subset of MAMP-Triggered Plant Responses

Previously, we demonstrated that *PARG2* (At2g31865) gene expression was up-regulated in response to flg22 treatment and during incompatible and compatible interactions with *Pst* DC3000 and its derivatives (Adams-Phillips et al., 2008). In this study, the regulation of *PARG2* during plant defense responses was further investigated. A robust up-regulation of *PARG2* gene expression was observed upon infection with the necrotrophic fungus *B. cinerea* and in the constitutive defense mutants *nudt7* and *cpr5-2* (Supplemental Fig. S2), supporting a role for *PARG2* in general plant defense responses. On the other hand, *PARG1* (At2g31870) gene expression was not significantly induced by *B. cinerea* (Supplemental Fig. S2) and was transiently induced 30 min after MAMP treatment (Supplemental Fig. S2).

T-DNA insertion lines disrupting the *PARG1* and *PARG2* genes were acquired, and reverse transcription (RT)-PCR was used to confirm reduction in expression of RNA for the appropriate loci (Supplemental Fig. S3). Similar to experiments with 3AB, we found that ROS production is not altered in *parg* mutants (Supplemental Fig. S3). MAMP-induced lignin and callose production also were not noticeably altered in *parg* mutants (data not shown). Seedling growth inhibition is used as a marker of innate immune responses in plants (Gomez-Gomez et al., 1999); growth inhibition is common in plants that have continuously activated defenses (Greenberg and Ausubel, 1993; Bowling et al., 1994; Yu et al., 1998). Notably, the response of *parg1* mutant plants to elf18 peptide in seedling growth inhibition assays is stronger (Fig. 4A), analogous to the exaggerated response to flg22 seen in wild-type seedlings treated with 3AB (Adams-Phillips et al., 2008). This was observed for two independent T-DNA insertion lines representing two different *parg1* mutant alleles (Supplemental Fig. S3). Coincident with the exaggerated seedling growth inhibition response, more elf18-induced pigment accumulates in *parg1* mutants compared with wild-type seedlings (Fig. 4B). It is also

Table 1. Callose response of Arabidopsis seedlings after flg22 treatment, with or without 3AB and SA treatment

+, Extensive callose deposition; –, little or no callose deposition. Callose deposition was monitored by microscopy after aniline blue staining in seedlings collected and fixed 24 h after flg22 treatment.

Genotype	flg22	flg22 + 3AB	flg22 + 3AB + SA
Wild type	+	–	+
<i>nahG</i> ⁺	+	–	+
<i>sid2</i>	+	–	+
<i>npr1</i>	+	–	+

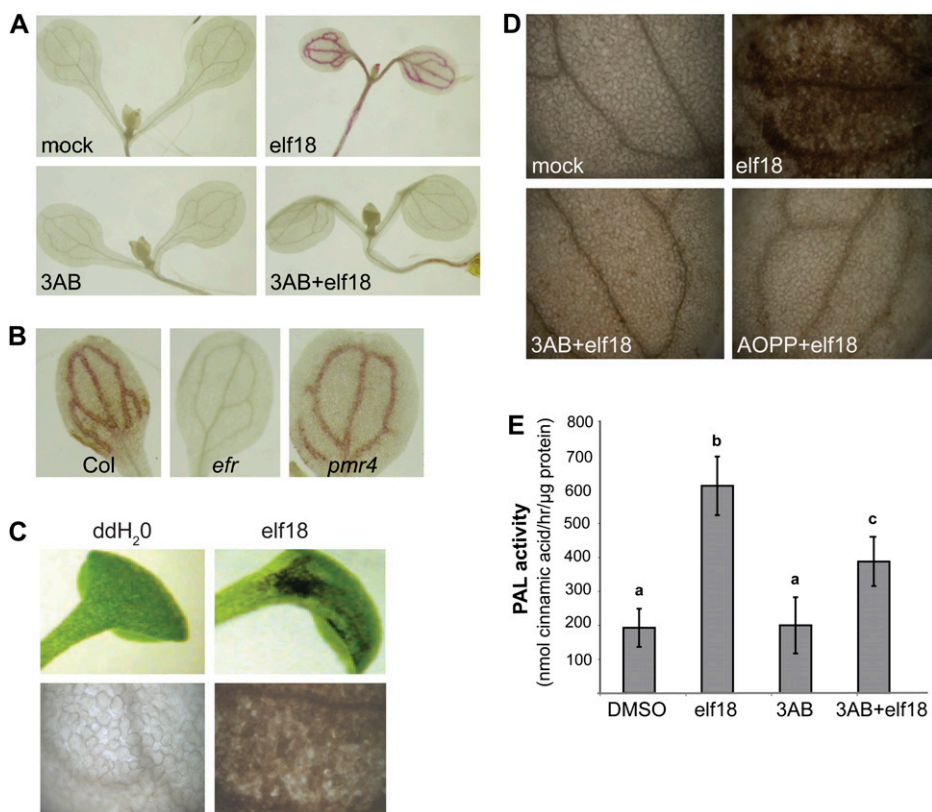


Figure 3. PARP inhibitor also disrupts MAMP-induced lignification and other aspects of the phenylpropanoid pathway. A, Guaiacyl lignin formation in wild-type Col-0 Arabidopsis seedlings mock treated (0.6% DMSO and distilled, deionized water) or treated with 2.5 mM 3AB followed by either distilled, deionized water or 0.5 μ M elf18 for 48 h, then fixed and stained with phloroglucinol. B, Guaiacyl lignin in Arabidopsis wild-type (Col), *efr* mutant (EF-Tu insensitive), and *pmr4* mutant (callose synthase) seedlings exposed to elf18 elicitor 48 h prior to staining as in A. C, Dark pigment in wild-type seedlings treated with distilled, deionized water (ddH₂O) or 2.5 μ M elf18 for 5 d. Leaves in the top panels were photographed in natural light (no fixing or staining), and leaves in the bottom panels were cleared in ethanol and then the area of leaf blade near the petiole was photographed (view is of approximately 100 leaf cells). D, Dark pigment in seedlings mock treated with 0.6% DMSO, 0.1 mM AOPP (PAL inhibitor) and 0.6% DMSO, or 2.5 mM 3AB prior to treatment with 2.5 μ M elf18 for 5 d, at which time leaves were cleared in ethanol and photographed. In A to D, photographs are representative of multiple replicate samples, and the experiments shown were repeated at least twice with similar results. E, PAL activity in 10-d-old Arabidopsis seedlings treated with 2.5 μ M elf18 and/or 5 mM 3AB. PAL activity was measured after 24 h. The graph presents results from three independent biological replicates (means \pm se). Bars with the same letter are not significantly different (one-way ANOVA; Tukey's simultaneous test; $P < 0.001$).

notable that *parg1* seedlings are hyperresponsive to the DNA-damaging agent mitomycin C (Fig. 4C). Even though *PARG2* (and not *PARG1*) expression is strongly induced by flg22 or elf18 treatment (Supplemental Figs. S2 and S3), it is the *parg1* mutant that exhibited the above alterations in response to defense-eliciting MAMPs. *parg2* mutants exhibited responses to elf18 and flg22 elicitation as well as to mitomycin C treatment that were not distinguishable from the response of wild-type plants (Fig. 4).

Disruption of PARG Gene Expression Potentiates Arabidopsis Susceptibility to the Necrotrophic Pathogen *B. cinerea*

In order to further characterize the role of *PARG* genes in plant defense responses, *parg* mutants were

tested for altered susceptibility to pathogens. No significant differences between the wild type and *parg* mutants were observed in limiting the growth of virulent and avirulent *Pst* DC3000 (Supplemental Fig. S4). In an experiment with multiple replicates but that to date has been performed only once, we also did not observe any alteration in the macroscopic hypersensitive response in *parg* mutants in response to avirulent *Pst* DC3000 or in 3AB-treated leaves in response to dexamethasone-induced expression of *avrRpt2* (Supplemental Table S1). However, in multiple experiments, both *parg1* and *parg2* knockdown plants displayed an accelerated onset of symptoms relative to wild-type plants after spray inoculation with *B. cinerea* spores (Fig. 5). This increased susceptibility was statistically significant, although not as severe as the susceptibility of *ein2-1* mutant plants (Fig. 5), which

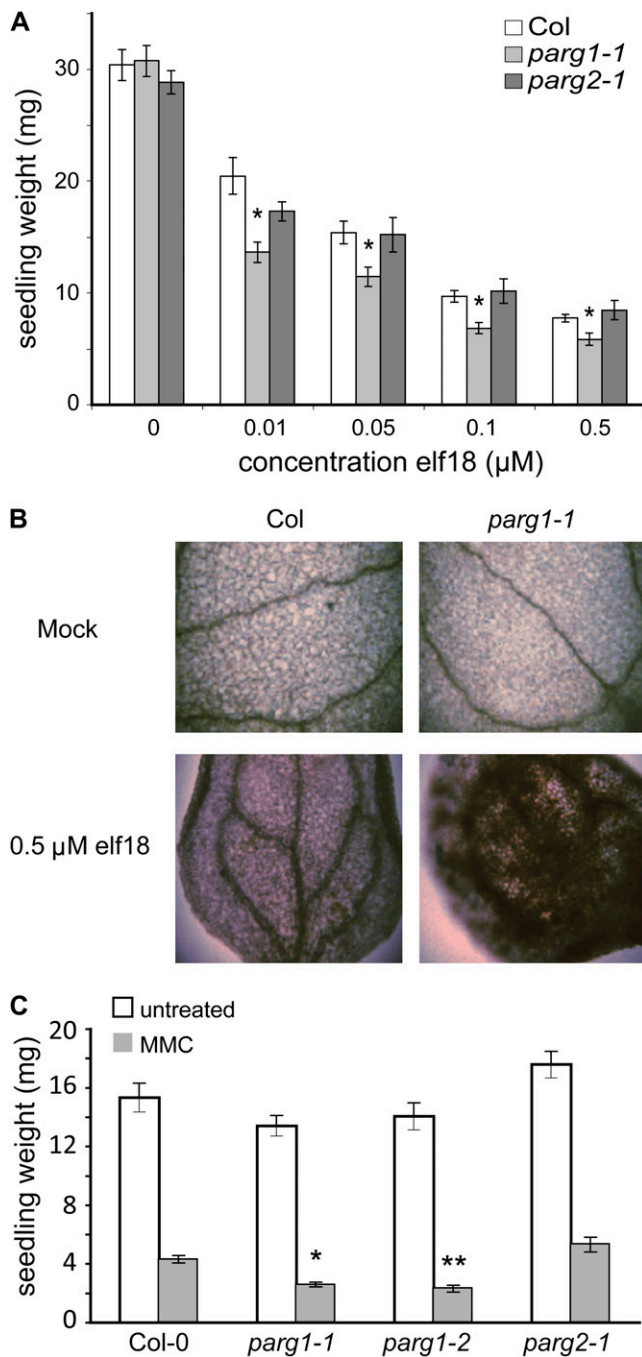


Figure 4. Excessive/aberrant response to MAMPs, and sensitivity to DNA damage, in *parG1* mutants. **A**, Seedling growth inhibition, a standard assay for plant responses to MAMPs. Five-day-old seedlings of the indicated genotypes were treated with the indicated concentrations of elf18 peptide and grown for an additional 7 d. Three separate experiments were performed, and a representative graph is shown; asterisks summarize ANOVA results across all experiments for tests of similarity of means between the mutant genotype and wild-type plants treated with the same concentration of elf18 (Tukey's simultaneous test: * $P < 0.001$; no asterisk, $P > 0.05$). A second mutant allele of *PARG1* was tested with similar results (Supplemental Fig. S3). **B**, Hyperaccumulation of MAMP-induced pigment in *parG1* mutant leaves (see also Fig. 3, C and D). Seedlings were fixed in FAA after 7 d of growth in the

are known to be hypersusceptible to this fungus (Thomma et al., 1999).

Interaction of Adult Arabidopsis with *Pst* DC3000 Leads to Activation of Cellular Poly(ADP-ribosyl)ation Reactions

In addition to inhibitor and mutant studies, direct biochemical assays were carried out to test for changes in poly(ADP-ribosyl)ation during plant responses to pathogens. Since PARP consumes NAD^+ to synthesize ADP-Rib units, an examination of cellular NAD^+ levels can be used as an indirect measure of poly(ADP-Rib) synthesis activities (Chen et al., 1994; Du et al., 2003; De Block et al., 2005; Ishikawa et al., 2009). Whereas no significant change in NAD^+ levels was seen for seedlings treated with avirulent pathogen, flg22 and/or 3AB (data not shown), a statistically significant 40% to 50% decrease in NAD^+ compared with mock-infiltrated samples was observed in leaves 12 h after infiltration with virulent *Pst* DC3000 (Supplemental Fig. S5). The decrease in NAD^+ concentrations observed by DeBlock et al. (2005) in Arabidopsis exposed to abiotic stresses such as high light was of a similar 50% magnitude. However, it is possible that the decrease in NAD^+ that we observed reflects perturbations in basic cellular mechanisms due to the progression of successful infection by a virulent pathogen, rather than reflecting the activation of an NAD^+ -consuming PARP enzymatic reaction. Therefore, we turned to immunodetection of poly(ADP-Rib) polymer levels as a more direct measure of PARP activation.

Poly(ADP-Rib) polymers and poly(ADP-ribosyl)ated protein species were monitored in seedlings treated with flg22 peptide as well as in adult Arabidopsis leaf tissue during interactions with virulent and avirulent *Pst* DC3000 strains and *B. cinerea* (Fig. 6; Supplemental Fig. S6). No significant changes in poly(ADP-Rib) levels were detected in flg22- or 3AB-treated seedlings (Supplemental Fig. S6), but both total cellular and nuclear poly(ADP-Rib) polymers increased somewhat in response to virulent *Pst* DC3000 and increased significantly (by 50%) in adult leaves treated with avirulent *Pst* DC3000 at 12 h post infection (hpi) relative to mock-treated leaves (Fig. 6A). DeBlock et al. (2005) observed a quantitatively similar increase in total polymer levels during abiotic (high-light) stress responses in Arabidopsis. We also observed a

presence of elf18 or solvent control, then cleared in ethanol and photographed. **C**, Sensitivity to the DNA-damaging agent mitomycin C (MMC). Wild-type (Col-0), *parG1-1*, *parG1-2*, and *parG2* seedlings were grown in the presence or absence of $40 \mu\text{M}$ mitomycin C for 10 d, and seedling weights were recorded. Asterisks summarize results across three experiments for ANOVA tests of similarity of means between wild-type and mutant plants for the same treatment (Tukey's simultaneous test: * $P < 0.01$; ** $P < 0.0001$). [See online article for color version of this figure.]

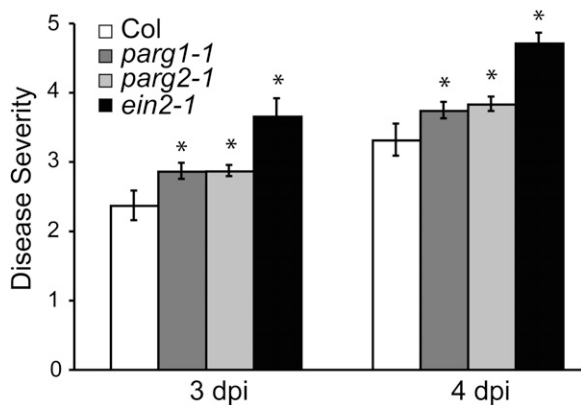


Figure 5. Loss of *PARG1* or *PARG2* gene expression increases susceptibility to *B. cinerea*. Disease symptom severity in wild-type (Col), *parg1-1*, *parg2-1*, or *ein2-1* plants 3 and 4 d after spraying with 1×10^5 *B. cinerea* spores mL^{-1} , as determined using a visual scale of 0 to 5 (0 = no symptoms, 1 = chlorosis, 2 = necrotic lesions present, 3 = necrotic lesions present on most leaves, 4 = hyphae visible to the naked eye, 5 = massive visible fungal growth). Means \pm SE are shown. * $P < 0.05$ for ANOVA tests of similarity of means between wild-type and mutant plants for data from four independent experiments. dpi, Days post inoculation.

2-fold increase in poly(ADP-Rib) polymer levels in positive control experiments that used high-light stress (data not shown).

When *Arabidopsis* leaf extracts were separated by SDS-PAGE, a poly(ADP-ribosyl)ated species migrating at an apparent mass of 43 kD was reproducibly 2- to 5-fold more abundant in both compatible and incompatible interactions with *Pst* DC3000 at 4 hpi than in mock-treated tissue (Fig. 6, B and C). The presence of low levels of this modified protein in mock-inoculated samples (Fig. 6C) supports the notion that it is an endogenous plant protein and not a bacterial protein present in both compatible and incompatible interactions. The 43-kD band detected by immunodetection methods (Fig. 6C) was not abundant enough to yield sufficient protein for mass spectrometry characterization in scaled-up experiments. Conversely, the abundance of a poly(ADP-ribosyl)ated doublet (approximately 50 kD) dramatically decreased over the first 2 d of infection with *B. cinerea* (Fig. 6D). Individually, poly(ADP-ribosyl)ated proteins were also monitored by SDS-PAGE in 14-d-old seedlings treated with flg22 or 3AB. No reproducibly detectable changes to individual modified protein species were observed, although the number of apparent poly(ADP-ribosyl)ated proteins was consistently much greater in seedlings than in adult leaves (Supplemental Fig. S6).

DISCUSSION

In this study, we used a combination of pharmacological inhibitors, genetic mutants, and biochemical

assays to examine the role of poly(ADP-ribosyl)ation during plant innate immune responses to MAMPs, biotrophic bacteria, and a necrotrophic fungus.

Poly(ADP-ribosyl)ation Regulates a Subset of Basal Immune Responses

While callose and lignin deposition responses are reduced after 3AB treatment, other MAMP-induced responses, such as ROS production and *WRKY29* and *FRK1* gene expression, remained unchanged (Fig. 1, B and C). Likewise, our analysis of *parg* mutants indicated that while knockout of *parg1* leads to hypersensitivity to elf18 treatment (exacerbated seedling growth inhibition and increased pigment production; Fig. 4, A and B), other MAMP-triggered responses such as the early ROS burst were not affected (Supplemental Fig. 3C). These and other findings demonstrate that poly(ADP-ribosyl)ation regulates a subset of plant basal immune responses.

As is also found in the animal literature (see introduction), during plant defense responses PARG seemingly acted to enhance the impacts of PARP activity or to counteract the impacts of PARP activity, depending on cellular context. 3AB treatment and *parg1* mutation both caused exaggerated seedling growth inhibition upon MAMP treatment, yet 3AB (and not *parg1* mutation) disrupted callose and lignin deposition, and *parg1* mutation (but not 3AB) caused elevated pigment production in response to elf18.

Poly(ADP-ribosyl)ation and MAMP-Elicited Plant Cell Wall Modifications

We previously reported that PARP inhibition blocks MAMP-induced callose deposition (Adams-Phillips et al., 2008). In this study, we found that PARP inhibition by 3AB specifically inhibits MAMP-elicited callose and not wound-induced callose or callose produced in *mekk1* mutants (Fig. 1). 3AB still blocked callose deposition if applied 5 h after initiation of innate immune signaling events. 3AB also blocked the production of lignin (Fig. 3A), a product of the phenylpropanoid pathway and another key component of pathogen-induced papillae. PARP inhibition also blocked production of an elf18-induced pigment that is presumed to derive in part from the phenylpropanoid pathway (since AOPP, a PAL inhibitor, also blocks this pigment production; Fig. 3D). We further determined that 3AB treatment can block activation of PAL in intact MAMP-elicited seedlings (Fig. 3E). PAL controls one of the first committed steps in the phenylpropanoid pathway, indicating that PARP likely has a global impact on numerous pathogenesis-induced products from the phenylpropanoid pathway.

This study contributes additional insight into the signaling networks that regulate MAMP-induced callose deposition (Kim et al., 2005; Clay et al., 2009). We found that the predominant signaling network that mediates flg22-elicited callose deposition is blocked by

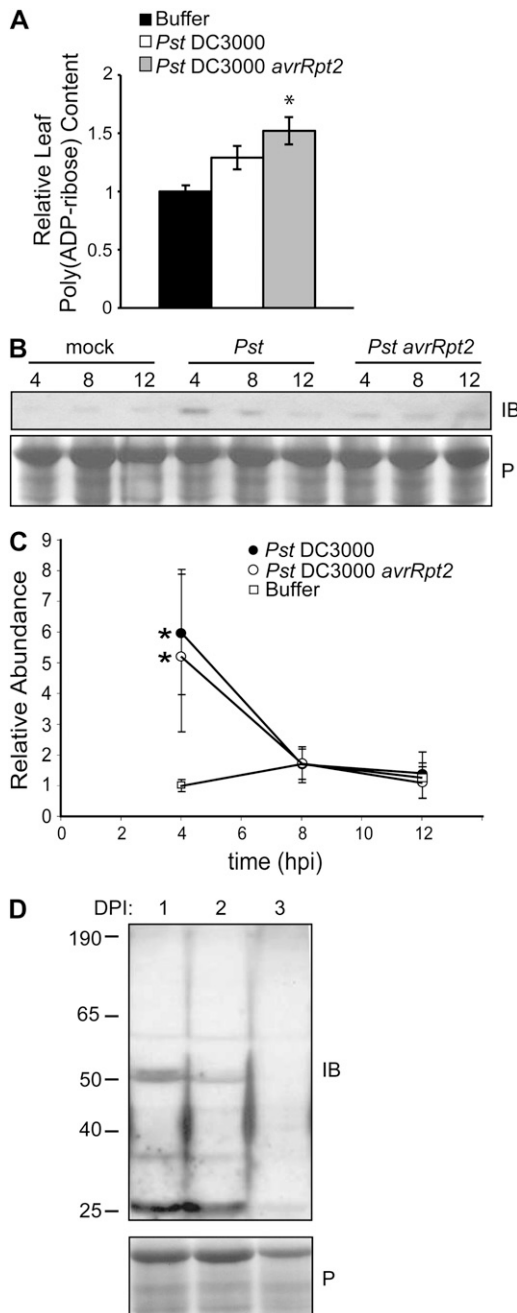


Figure 6. Poly(ADP-ribosyl)ation is activated by pathogen attack. **A**, Total cellular ADP-Rib polymer abundance in Col-0 plants 12 h after infiltration with virulent (DC3000) or avirulent (DC3000 *avrRpt2*) *Pst* DC3000 relative to mock-treated (buffer) plants. ADP-Rib polymer levels were quantified by immuno-dot blot and image analysis software. Means \pm SE are shown for intensity levels normalized to intensity for mock-treated material within same experiment. * $P < 0.001$ for ANOVA (Tukey's simultaneous test for similarity of means between pathogen-treated and mock-inoculated plants) for five separate experiments. **B**, Original image of a representative experiment, monitoring poly(ADP-ribosyl)ation of a 43-kD protein species detected by immunoblot (IB) analysis using anti-poly(ADP-Rib) antibody after Ponceau S (P) staining. **C**, Quantification for three immunoblot experiments (Tukey's simultaneous test; * $P < 0.001$). **D**, SDS-PAGE and immunoblot (IB) analysis of poly(ADP-ribosyl)ated proteins in Col-0 plants

PARP inhibitor. That network apparently can function independent of SA because *flg22*-induced callose deposition still occurs in *sid2* mutants or in plants expressing *nahG*⁺ as well as in *npr1* mutants (Table I). However, there appears to be a *flg22*-responsive branch in the callose signaling pathway that potentiates SA-responsive callose deposition. SA alone does not induce callose deposition, but *flg22* + SA does, indicating that *flg22* potentiates SA-responsive callose deposition. SA or BTH feeding can bypass 3AB inhibition of *flg22*-induced callose deposition, suggesting that 3AB does not block the *flg22*-potentiated SA-responsive branch of the network. Hence, it seems likely that there is a separate portion of the signaling network, leading from *flg22* perception to potentiation of SA-responsive/NPR1-independent callose deposition, that PARP inhibitor does not block. PARP inhibition by 3AB also did not alter *flg22*-induced *MYB51* or *CYP81F2* gene expression (Fig. 2A), which Clay et al. (2009) had previously shown are induced as part of the distinct ethylene/*MYB51*-dependent and *CYP81F2*-dependent pathways that are required for *flg22*-induced callose deposition. Our data, therefore, additionally suggest that 3AB blockage of MAMP-induced callose is independent of and/or downstream of the *MYB51*/ethylene-dependent and *CYP81F2*/I3G-dependent portions of these networks.

We found that chemical PARP inhibition blocks components of the phenylpropanoid pathway, which raises experimentally challenging questions as to how this impacts responses to plant pathogens. There are two proposed pathways for SA biosynthesis in plants: through isochlorismate synthase and through the phenylpropanoid pathway (Mauch-Mani and Slusarenko, 1996; Wildermuth et al., 2001). In future work, it may be of interest to test if PARP is impacting one or the other source of SA. Besides SA, other products of the phenylpropanoid pathway include ROS scavengers. Vitamin C-deficient mutants (*vtc1*) impaired in ROS scavenging activities exhibit reduced MAMP-induced callose production that can be rescued by SA treatment (Clay et al., 2009), similar to our experiments with 3AB (Fig. 2B). We observed no alteration in MAMP-elicited ROS production in the first half hour after treatment with PARP inhibitor (Fig. 1B), indicating that poly(ADP-ribosyl)ation does not regulate the deposition of cell wall reinforcement compounds such as callose and lignin by regulating early ROS burst events after defense elicitation. However, it remains possible that poly(ADP-ribosyl)ation can at some secondary or tertiary level alter defense-associated ROS levels and/or the response to those ROS, such as by causing shifts in phenylpropanoid metabolites that alter ROS scavenging.

sampled at 1 (lane 1), 2 (lane 2), and 3 (lane 3) d post inoculation (DPI) after spraying with 1×10^5 spores mL^{-1} *B. cinerea*. Blots were stained with Ponceau S before immunoblotting.

Activation of Cellular Poly(ADP-ribosyl)ation Reactions in Response to Pathogen Infection

When we examined total ADP-Rib polymer levels in plants inoculated with different strains of *Pst* DC3000, we found a significant increase in total ADP-Rib polymer 12 h after infection in plants inoculated with avirulent but not virulent pathogen (Fig. 6A). This observation provides further evidence of the previously unknown association between poly(ADP-ribosyl)ation and plant responses to pathogens. Free ADP-Rib polymer is a known cell death signal in animal cells, acting at the mitochondria to stimulate release of apoptosis-inducing factor (Heeres and Hergenrother, 2007; David et al., 2009), but in initial experiments, we have not observed an overt change in the severity or rate of development of macroscopic *avrRpt2*-elicited hypersensitive response symptoms in *parg1* and *parg2* mutants or with 3AB treatment (Supplemental Table S1). However, given the findings regarding apoptosis and poly(ADP-Rib) in animal systems, our detection of elevated ADP-Rib polymer during an incompatible interaction suggests that, in the future, a study of the possible role of ADP-Rib polymer in plants responding to avirulent pathogen may be warranted. In addition, although *parg* mutants showed no macroscopic changes in their interaction with biotrophic *Pst* DC3000 (Supplemental Fig. S4), these same mutants were more susceptible to the necrotrophic pathogen *B. cinerea* (Fig. 5). Arabidopsis *parg* mutants are known to accumulate ADP-Rib polymers (Panda et al., 2002), but future studies will be required to investigate causal relationships of poly(ADP-Rib) polymer accumulation and the observed increase in susceptibility to necrotrophic pathogens.

We also observed significant accumulation of a discrete poly(ADP-ribosyl)ated protein species in response to virulent and avirulent *Pst* DC3000 at 4 hpi (Fig. 6, B and C). From these experiments, we conclude that poly(ADP-ribosyl)ation of at least one target protein occurs as an initial response to contact with *Pst* DC3000. We also detected significantly decreased abundance of a poly(ADP-ribosyl)ated protein over the first 2 d of infection with *B. cinerea* (Fig. 6D), indicating the dynamic nature of PARP activity during two very different types of plant-pathogen interactions.

Despite the observed increase in ADP-Rib polymer and protein poly(ADP-ribosyl)ation in response to avirulent *Pst* DC3000, NAD⁺ levels at 4, 8, and 12 h did not detectably change in adult plants inoculated with avirulent pathogen (Supplemental Fig. S5). Depletion of NAD⁺ pools is suggested to be significant in plant abiotic stress and for some animal systems (Du et al., 2003; De Block et al., 2005). We cannot exclude the possibility that the methods we used to detect NAD⁺ and ADP-Rib polymer were not sensitive enough to detect more subtle or transient yet significant changes. However, the results of this study suggest that PARP activation does not affect plant defense through significant depletion of NAD⁺ pools after activation of PARP enzyme.

NUDT7 Biotic Stress Findings Also Implicate Poly(ADP-ribosyl)ation

Recent findings from other studies have shown impacts of Arabidopsis NUDT7 on biotic stress responses (Bartsch et al., 2006; Jambunathan and Mahalingam, 2006; Ge et al., 2007; Adams-Phillips et al., 2008). Although not demonstrably tied to poly(ADP-ribosyl)ation at the time, those findings further suggest possible impacts of poly(ADP-ribosyl)ation on plant responses to pathogens, especially in light of this report and recent results showing direct impacts of NUDT7 on plant poly(ADP-ribosyl)ation (Ishikawa et al., 2009). However, because NUDT7 action has multiple physiological impacts (see introduction), there are varied mechanisms through which NUDT7 may be impacting plant responses to biotic stress, and only some of them directly involve poly(ADP-ribosyl)ation. For example, the defense phenotypes of *nudt7* mutants may be due to accumulation of free ADP-Rib, which may induce stress responses, or may be due to alterations in NADH hydrolysis rather than ADP-Rib hydrolysis (Ge et al. 2007).

Poly(ADP-ribosyl)ation at the Intersection between Plant Defense and DNA Repair

In animal systems, PARP is most prominent as a DNA break sensor and DNA repair pathway signaling molecule. DNA strand breaks are known to activate the expression and activity of PARP enzymes in plants (Babychuk et al., 1998; Doucet-Chabeaud et al., 2001; Chen et al., 2003). While pathogen-induced ROS production in plants contributes positively to disease resistance in a number of ways (Levine et al., 1994; Wojtaszek, 1997; Neill et al., 2002; Apel and Hirt, 2004), these same ROS can also oxidize DNA, creating a genotoxic challenge that the host must respond to. Therefore, by activating appropriate DNA repair pathways (Ishikawa et al., 2009) and protective mechanisms, poly(ADP-ribosyl)ation may be an important response to ROS production during defense. Phenylpropanoid pathway products can function in plant defense as ROS scavengers and as protective UV light-absorbing pigments or "sunscreen" that protect DNA from UV light-induced free radicals (superoxide, singlet oxygen, and hydroxyl radicals; Bieza and Lois, 2001; Filkowski et al., 2004; Ferrer et al., 2008). We observed that knockout of *parg1* leads to hyperaccumulation of a phenylpropanoid-derived pigment in response to *elf18* treatment (Fig. 4B) and that these same mutants are also more sensitive to the DNA-damaging agent mitomycin C (Fig. 4C). It is possible, therefore, that there are interactions between poly(ADP-ribosyl)ation, regulation of phenylpropanoid pathway activity, and protection of the genome from genotoxic stress.

DNA repair pathways may also be engaged during plant defense responses for reasons other than as a response to genotoxic stress. Pathogen stresses, such as *flg22* peptide and viral pathogen, increase somatic

homologous recombination frequency and cause DNA breaks that require subsequent repair (Lucht et al., 2002; Kovalchuk et al., 2003; Molinier et al., 2006). These and other observations suggest a link between homologous recombination and effective plant defense (Durrant et al., 2007; Friedman and Baker, 2007). Since PARP is activated by DNA breaks, and because PARP inhibitor disrupts innate immune responses (as described here) and elicits somatic homologous recombination (Puchta et al., 1995; Lucht et al., 2002; Filkowski et al., 2004; A.G. Briggs and A.F. Bent, unpublished data), poly(ADP-ribosyl)ation may be involved in such recombination mechanisms.

In summary, this study shows that PARP inhibitors and *parg* mutants alter specific plant responses to elicitation by pathogens and that ADP-Rib polymer levels change during infection. Our results suggest that poly(ADP-ribosyl)ation is a component of the response to multiple different biotic stresses in plants. Poly(ADP-ribosyl)ation may contribute to protection against genotoxic stress, to genome recombination, or to pathogen-induced host cell death; these possible protective activities require further investigation. However, it is clear from the data presented that poly(ADP-ribosyl)ation is involved in defense-associated cell wall reinforcement and in the response to infection by *B. cinerea*.

MATERIALS AND METHODS

Plant Lines and Growing Conditions

Arabidopsis (*Arabidopsis thaliana* accession Columbia [Col-0]) plants were grown at 22°C under short-day conditions (9 h of light/15 h of dark, 100–150 $\mu\text{mol m}^{-2} \text{s}^{-1}$) at a density of 16 seeds per 81 cm^2 . Aseptically grown *Arabidopsis* seedlings were obtained from surface-sterilized seeds germinated on 0.5× Murashige and Skoog agar medium with 2% (w/v) Suc and 1× Gamborg's vitamins for 5 d. Seedlings were then transferred to liquid 0.5× Murashige and Skoog salts, 1.5% (w/v) Suc, and 1× Gamborg's vitamins medium on 24-well plates for further analysis.

The homozygous T-DNA knockout lines *parg1-1* (SALK_147805), *parg1-2* (SALK_116088), *parg2* (GABI_072B04), and *nudt7* (SALK_0464410), all in the Col-0 background, were identified as described (Alonso et al., 2003; Rosso et al., 2003). *pmr4-1* (CS3858), *ein2-1* (CS3071), *cpr5-2* (CS3770), and chalcone synthase *tt-4* (CS85) mutant seeds were obtained from the *Arabidopsis* Biological Resource Center stock center; transgenic dex:*avrRpt2* plants (McNellis et al., 1998) were courtesy of B. Staskawicz (University of California-Berkeley), and *mekk1* seeds were kindly provided by P. Krysan (University of Wisconsin-Madison).

Pst DC3000 Culture and Plant Inoculations

Pseudomonas syringae pv *tomato* strain DC3000 carrying the plasmid pVSP61 with no insert or with *avrRpt2* under the control of its native promoter (Kunkel et al., 1993) was grown for 2 d on NYGA solid medium (5 g/L bacto-peptone, 3 g/L yeast extract, 20 mL/L glycerol, and 15 g/L agar) at 28°C. *Arabidopsis* plants (4–6 weeks old) were vacuum infiltrated with bacteria resuspended in 10 mM MgCl_2 at 1×10^7 colony-forming units mL^{-1} . Rosette leaves were collected by cutting with a razor at the basal stem at 4 to 12 hpi.

Bacterial growth in leaves was quantified at 3 d post inoculation with 1×10^5 colony-forming units mL^{-1} using standard procedures (Suarez-Rodriguez et al., 2007). In each experiment, leaf punches from four leaves were pooled and tested by dilution plating for each data point, with four data points per treatment.

Botrytis cinerea Culture and Inoculation

Botrytis cinerea (a gift of T. Mengiste, Purdue University) was grown on 0.5× V8-agar plates for 14 d in the dark at 22°C. Spores (1×10^5 spores mL^{-1}) were resuspended in Sabouraud's 10% maltose broth. *Arabidopsis* plants (4–6 weeks old) were sprayed with a fine mist of spore suspension and incubated under domes under standard growing conditions for 3 to 5 d post inoculation. Disease symptoms were determined using a 0 to 5 visual scale (0 = no symptoms, 1 = chlorosis, 2 = necrotic lesions present, 3 = necrotic lesions present on most leaves, 4 = hyphae visible to the naked eye, 5 = massive visible fungal growth). Disease rating by separate investigators after masking of genotype/treatment information gave highly consistent scoring data.

RNA Extraction and Gene Expression Analysis

Total RNA was extracted from leaf or seedling tissue (RNeasy Plant Mini Kit; Qiagen). Contaminating DNA was removed with an RNase-free DNase Set (Qiagen), and RNA concentrations were quantified by Nanodrop Spectrophotometer (Thermo Scientific). Semiquantitative RT-PCR was confirmed to be using a nonsaturating number of PCR cycles; reactions contained cDNA (synthesized with SuperScript III reverse transcriptase; Invitrogen), template, and corresponding gene-specific primers pairs: 5'-ATGGACGAAGGAGACCTAG-3' and 5'-CTTTCTTTGATTTGGATTCTG-3' (*WRKY29*); 5'-TACTATTGCGACTCGCCAAATG-3' and 5'-CTACCTTGTCTCGAGGAACC-3' (*FRK1*); 5'-AGGTTCGTGTCAGCCATC-3' and 5'-TTAGAAGCATTCTCTGTAAC-3' (*Actin-2*); 5'-CTCATGCTCAGTATGATGC-3' and 5'-CTCCAATCTTCTCGTCTATC-3' (*CYP81F2*); 5'-ACAAATGGTCTGCTATAGCT-3' and 5'-CTTGTGTGTAACCTGATCAA-3' (*MYB51*); 5'-TGCTTCCCAGACTCGAAGAC-3' and 5'-AGGCGGTGGATAGCTTTGTTGG-3' (*PARG1*); and 5'-ATATGCTCACTGCACGAAG-3' and 5'-GGTAGACAGTGAGGTCATGAGCC-3' (*PARG2*).

Seedling Growth Inhibition Assays

Seedlings were treated with varying concentrations of elicitor, as described above, and fresh weight was recorded 10 to 14 d later for eight to 12 seedlings per treatment.

Cell Wall Component Analysis

One day after transfer to liquid medium, seedlings were treated with varying concentrations of different chemicals and MAMP elicitors as noted. To induce a broad wounding response, cotyledons were squeezed with a pair of forceps. To induce a localized wound response, cotyledons were punctured with a sharp needle. For callose analysis, seedlings were fixed in formaldehyde/acetic acid/alcohol (FAA) for 24 h, cleared in ethanol, and stained with 0.01% aniline blue as described (Gomez-Gomez et al., 1999). A minimum of 12 cotyledons per condition per experiment were visualized under UV light with an epifluorescence microscope. For guaiacyl lignin analysis, 6-d-old seedlings were fixed in FAA at 48 hpi, cleared in ethanol, stained with 1:1 solution of 2% phloroglucinol and concentrated HCl, and photographed within 15 min of phloroglucinol staining (Newman et al., 2004).

ROS Assay

ROS were quantified using a luminol-based assay (Gomez-Gomez et al., 1999). Briefly, eight to 12 leaf discs per treatment were floated in 0.5% dimethyl sulfoxide (DMSO) overnight on a 96-well plate. Discs were treated with 0.6% DMSO or 2.5 mM 3AB for 30 min before addition of 0.1 mg mL^{-1} luminol (Fluka) and 0.1 mg mL^{-1} horseradish peroxidase (Sigma). Distilled, deionized water or 1.0 μM elf18 or flg22 was then added, and luminescence was measured approximately once per minute with a Synergy HT Multidetection Microplate Reader (BioTek). ROS data are presented as area under the luminescence curve during the first 30 min after elicitation, with area under the curve for each disc normalized to the mean area for the control samples tested within the same experiment.

Immunological Detection and Quantification of Poly(ADP-Rib)

Concentrations of total protein (CellLytic P extraction buffer; Sigma) and nuclear protein (CellLytic PN kit; Sigma) extracts treated with 1:100 plant

tissue culture protease inhibitor cocktail (Sigma) were quantified using bicinchoninic acid protein assay reagents (Bio-Rad). Total poly(ADP-Rib) polymer was quantified by dot blot as described (De Block et al., 2005; Hunt et al., 2007) using rabbit polyclonal anti-poly(ADP-Rib) primary antibody (Trevigen). Poly(ADP-ribosyl)ated proteins were analyzed by SDS-PAGE and immunoblot using the same rabbit polyclonal primary antibody, horseradish peroxidase-conjugated goat anti-rabbit secondary antibody (Bio-Rad), and detected using enhanced chemiluminescence reagents (GE Healthcare). Equal gel loading was confirmed by Ponceau S (Sigma) staining prior to immunoblotting.

NAD⁺ Quantification

Total cellular NAD⁺ concentrations were quantified from adult leaf or seedling tissue using an alcohol dehydrogenase-based colorimetric enzyme cycling assay, as described (Jacobson and Jacobson, 1976). A purified NAD⁺ standard curve was used, and all data points were adjusted to total cellular protein concentrations, as determined by bicinchoninic acid protein assay (Bio-Rad).

PAL Activity Assays

PAL activity was measured as described (Olsen et al., 2008). Briefly, 30 10-d-old *Arabidopsis* seedlings were treated with inhibitor and/or elicitor as described and harvested at 24 hpi. Treated tissue was ground and passed through a Sephadex G-25 column (GE Healthcare Life Sciences). PAL activity was measured from eluate as L-Phe converted to trans-cinnamic acid per hour (A₂₉₀; Saunders and McClure, 1974). Blanks were made similarly, except for the addition of HCl to a final concentration of 0.25 M prior to the addition of L-Phe. Bradford assays (Sigma) were performed on extracts to quantify protein, and results were expressed as nanomoles of trans-cinnamic acid formed per milligram of plant protein per hour.

Supplemental Data

The following materials are available in the online version of this article.

Supplemental Figure S1. Dose response of callose deposition in presence of PARP inhibitor.

Supplemental Figure S2. RT-PCR to monitor *PARG* gene expression.

Supplemental Figure S3. *parg* mutant characterization.

Supplemental Figure S4. Bacterial growth in *parg* mutants.

Supplemental Figure S5. NAD⁺ concentrations after infections by *P. syringae* pv *tomato*.

Supplemental Figure S6. Polymer levels and poly(ADP-ribosyl)ated proteins following biotic stress.

Supplemental Table S1. Hypersensitive response of *parg* mutants and in presence of PARP inhibitor.

ACKNOWLEDGMENTS

We thank Antonia Phillip and Sophia Zebell for their contributions to the experiments reported in this paper, Laura Helft for critically reading the manuscript, and the *Arabidopsis* Biological Resource Center and GABI-Kat for provision of *Arabidopsis* mutant lines.

Received September 25, 2009; accepted October 30, 2009; published November 4, 2009.

LITERATURE CITED

Adams-Phillips L, Wan J, Tan X, Dunning FM, Meyers BC, Michelmore RW, Bent AF (2008) Discovery of ADP-ribosylation and other plant defense pathway elements through expression profiling of four different *Arabidopsis*-*Pseudomonas* *R-avr* interactions. *Mol Plant Microbe Interact* **21**: 646–657

Ahel D, Horejsi Z, Wiechens N, Polo SE, Garcia-Wilson E, Ahel I, Flynn H, Skehel M, West SC, Jackson SP, et al (2009) Poly(ADP-ribose)-

dependent regulation of DNA repair by the chromatin remodeling enzyme ALC1. *Science* **325**: 1240–1243

Alonso JM, Stepanova AN, Leisse TJ, Kim CJ, Chen H, Shinn P, Stevenson DK, Zimmerman J, Barajas P, Cheuk R, et al (2003) Genome-wide insertional mutagenesis of *Arabidopsis thaliana*. *Science* **301**: 653–657

Ame JC, Apiou F, Jacobson EL, Jacobson MK (1999) Assignment of the poly(ADP-ribose) glycohydrolase gene (*PARG*) to human chromosome 10q11.23 and mouse chromosome 14B by in situ hybridization. *Cytogenet Cell Genet* **85**: 269–270

Amor Y, Babiychuk E, Inze D, Levine A (1998) The involvement of poly(ADP-ribose) polymerase in the oxidative stress responses in plants. *FEBS Lett* **440**: 1–7

Andrabi SA, Kim NS, Yu SW, Wang H, Koh DW, Sasaki M, Klaus JA, Otsuka T, Zhang Z, Koehler RC, et al (2006) Poly(ADP-ribose) (PAR) polymer is a death signal. *Proc Natl Acad Sci USA* **103**: 18308–18313

Apel K, Hirt H (2004) Reactive oxygen species: metabolism, oxidative stress, and signal transduction. *Annu Rev Plant Biol* **55**: 373–399

Asai T, Tena G, Plotnikova J, Willmann MR, Chiu WL, Gomez-Gomez L, Boller T, Ausubel FM, Sheen J (2002) MAP kinase signalling cascade in *Arabidopsis* innate immunity. *Nature* **415**: 977–983

Babiychuk E, Cottrill PB, Storozhenko S, Fuangthong M, Chen Y, O'Farrell MK, Van Montagu M, Inze D, Kushnir S (1998) Higher plants possess two structurally different poly(ADP-ribose) polymerases. *Plant J* **15**: 635–645

Bartsch M, Gobatto E, Bednarek P, Debey S, Schultze JL, Bautor J, Parker JE (2006) Salicylic acid-independent ENHANCED DISEASE SUSCEPTIBILITY1 signaling in *Arabidopsis* immunity and cell death is regulated by the monooxygenase *FMO1* and the Nudix hydrolase *NUDT7*. *Plant Cell* **18**: 1038–1051

Beauchamp MC, Knafo A, Yasmeen A, Carboni JM, Gottardis MM, Pollak MN, Gottlieb WH (2009) BMS-536924 sensitizes human epithelial ovarian cancer cells to the PARP inhibitor, 3-aminobenzamide. *Gynecol Oncol* **115**: 193–198

Bent AF, Mackey D (2007) Elicitors, effectors, and R genes: the new paradigm and a lifetime supply of questions. *Annu Rev Phytopathol* **45**: 399–436

Berglund T, Kalbin G, Strid A, Rydstrom J, Ohlsson AB (1996) UV-B- and oxidative stress-induced increase in nicotinamide and trigonelline and inhibition of defensive metabolism induction by poly(ADP-ribose)polymerase inhibitor in plant tissue. *FEBS Lett* **380**: 188–193

Bestwick CS, Bennett MH, Mansfield JW (1995) Hrp mutant of *Pseudomonas syringae* pv *phaseolicola* induces cell wall alterations but not membrane damage leading to the hypersensitive reaction in lettuce. *Plant Physiol* **108**: 503–516

Bestwick CS, Brown IR, Bennett MH, Mansfield JW (1997) Localization of hydrogen peroxide accumulation during the hypersensitive reaction of lettuce cells to *Pseudomonas syringae* pv *phaseolicola*. *Plant Cell* **9**: 209–221

Bhuiyan NH, Selvaraj G, Wei Y, King J (2009) Role of lignification in plant defense. *Plant Signal Behav* **4**: 158–159

Bieza K, Lois R (2001) An *Arabidopsis* mutant tolerant to lethal ultraviolet-B levels shows constitutively elevated accumulation of flavonoids and other phenolics. *Plant Physiol* **126**: 1105–1115

Bowling SA, Guo A, Cao H, Gordon AS, Klessig DF, Dong X (1994) A mutation in *Arabidopsis* that leads to constitutive expression of systemic acquired resistance. *Plant Cell* **6**: 1845–1857

Brown I, Trethowan J, Kerry M, Mansfield J, Bolwell GP (1998) Localization of components of the oxidative cross-linking of glycoproteins and of callose synthesis in papillae formed during the interaction between non-pathogenic strains of *Xanthomonas campestris* and French bean mesophyll cells. *Plant J* **15**: 333–344

Bryant HE, Schultz N, Thomas HD, Parker KM, Flower D, Lopez E, Kyle S, Meuth M, Curtin NJ, Helleday T (2005) Specific killing of BRCA2-deficient tumours with inhibitors of poly(ADP-ribose) polymerase. *Nature* **434**: 913–917

Chen IP, Haehnel U, Altschmied L, Schubert I, Puchta H (2003) The transcriptional response of *Arabidopsis* to genotoxic stress: a high-density colony array study (HDCA). *Plant J* **35**: 771–786

Chen YM, Shall S, O'Farrell M (1994) Poly(ADP-ribose) polymerase in plant nuclei. *Eur J Biochem* **224**: 135–142

Clay NK, Adio AM, Denoux C, Jander G, Ausubel FM (2009) Glucosinolate metabolites required for an *Arabidopsis* innate immune response. *Science* **323**: 95–101

- David KK, Andrabi SA, Dawson TM, Dawson VL (2009) Parthanatos, a messenger of death. *Front Biosci* **14**: 1116–1128
- Davidovic L, Vodenicharov M, Affar EB, Poirier GG (2001) Importance of poly(ADP-ribose) glycohydrolase in the control of poly(ADP-ribose) metabolism. *Exp Cell Res* **268**: 7–13
- De Block M, Verduyn C, De Brouwer D, Cornelissen M (2005) Poly(ADP-ribose) polymerase in plants affects energy homeostasis, cell death and stress tolerance. *Plant J* **41**: 95–106
- DeRoy S, Thilmony R, Kwack YB, Nomura K, He SY (2004) A family of conserved bacterial effectors inhibits salicylic acid-mediated basal immunity and promotes disease necrosis in plants. *Proc Natl Acad Sci USA* **101**: 9927–9932
- de Torres M, Mansfield JW, Grabov N, Brown IR, Ammoun H, Tsiamis G, Forsyth A, Robatzek S, Grant M, Boch J (2006) *Pseudomonas syringae* effector AvrPtoB suppresses basal defence in *Arabidopsis*. *Plant J* **47**: 368–382
- Ding W, Liu W, Cooper KL, Qin XJ, de Souza Bergo PL, Hudson LG, Liu KJ (2009) Inhibition of poly(ADP-ribose) polymerase-1 by arsenite interferes with repair of oxidative DNA damage. *J Biol Chem* **284**: 6809–6817
- Doucet-Chabeaud G, Godon C, Brutesco C, de Murcia G, Kazmaier M (2001) Ionising radiation induces the expression of PARP-1 and PARP-2 genes in *Arabidopsis*. *Mol Genet Genomics* **265**: 954–963
- Du L, Zhang X, Han YY, Burke NA, Kochanek PM, Watkins SC, Graham SH, Carcillo JA, Szabo C, Clark RS (2003) Intra-mitochondrial poly(ADP-ribosylation) contributes to NAD⁺ depletion and cell death induced by oxidative stress. *J Biol Chem* **278**: 18426–18433
- Durrant WE, Wang S, Dong X (2007) *Arabidopsis* SN1 and RAD51D regulate both gene transcription and DNA recombination during the defense response. *Proc Natl Acad Sci USA* **104**: 4223–4227
- Ferrer JL, Austin MB, Stewart C Jr, Noel JP (2008) Structure and function of enzymes involved in the biosynthesis of phenylpropanoids. *Plant Physiol Biochem* **46**: 356–370
- Feys BJ, Parker JE (2000) Interplay of signaling pathways in plant disease resistance. *Trends Genet* **16**: 449–455
- Filkowski J, Kovalchuk O, Kovalchuk I (2004) Genome stability of *vtc1*, *tt4*, and *tt5* *Arabidopsis thaliana* mutants impaired in protection against oxidative stress. *Plant J* **38**: 60–69
- Friedman AR, Baker BJ (2007) The evolution of resistance genes in multi-protein plant resistance systems. *Curr Opin Genet Dev* **17**: 493–499
- Ge X, Li GJ, Wang SB, Zhu H, Zhu T, Wang X, Xia Y (2007) AtNUDT7, a negative regulator of basal immunity in *Arabidopsis*, modulates two distinct defense response pathways and is involved in maintaining redox homeostasis. *Plant Physiol* **145**: 204–215
- Gomez-Gomez L, Felix G, Boller T (1999) A single locus determines sensitivity to bacterial flagellin in *Arabidopsis thaliana*. *Plant J* **18**: 277–284
- Grant M, Mansfield J (1999) Early events in host-pathogen interactions. *Curr Opin Plant Biol* **2**: 312–319
- Greenberg JT, Ausubel FM (1993) *Arabidopsis* mutants compromised for the control of cellular damage during pathogenesis and aging. *Plant J* **4**: 327–341
- Hammond-Kosack KE, Parker JE (2003) Deciphering plant-pathogen communication: fresh perspectives for molecular resistance breeding. *Curr Opin Biotechnol* **14**: 177–193
- Hanai S, Kanai M, Ohashi S, Okamoto K, Yamada M, Takahashi H, Miwa M (2004) Loss of poly(ADP-ribose) glycohydrolase causes progressive neurodegeneration in *Drosophila melanogaster*. *Proc Natl Acad Sci USA* **101**: 82–86
- Hashida SN, Takahashi H, Uchimiya H (2009) The role of NAD biosynthesis in plant development and stress responses. *Ann Bot (Lond)* **103**: 819–824
- Hassa PO, Hottiger MO (2008) The diverse biological roles of mammalian PARPs, a small but powerful family of poly-ADP-ribose polymerases. *Front Biosci* **13**: 3046–3082
- Hauck P, Thilmony R, He SY (2003) A *Pseudomonas syringae* type III effector suppresses cell wall-based extracellular defense in susceptible *Arabidopsis* plants. *Proc Natl Acad Sci USA* **100**: 8577–8582
- Heeres JT, Hergenrother PJ (2007) Poly(ADP-ribose) makes a date with death. *Curr Opin Chem Biol* **11**: 644–653
- Hernandez AI, Wolk J, Hu JY, Liu J, Kurosu T, Schwartz JH, Schacher S (2009) Poly-(ADP-ribose) polymerase-1 is necessary for long-term facilitation in *Aplysia*. *J Neurosci* **29**: 9553–9562
- Huletsky A, de Murcia G, Muller S, Hengartner M, Menard L, Lamarre D, Poirier GG (1989) The effect of poly(ADP-ribosyl)ation on native and H1-depleted chromatin: a role of poly(ADP-ribosyl)ation on core nucleosome structure. *J Biol Chem* **264**: 8878–8886
- Hunt L, Holdsworth MJ, Gray JE (2007) Nicotinamidase activity is important for germination. *Plant J* **51**: 341–351
- Hunt L, Lerner F, Ziegler M (2004) NAD: new roles in signalling and gene regulation in plants. *New Phytol* **163**: 31–44
- Ishikawa K, Ogawa T, Hirose E, Nakayama Y, Harada K, Fukusaki E, Yoshimura K, Shigeoka S (2009) Modulation of the poly(ADP-ribosyl)ation reaction via the *Arabidopsis* ADP-ribose/NADH pyrophosphohydrolase, AtNUDX7, is involved in the response to oxidative stress. *Plant Physiol* **151**: 741–754
- Jacobs AK, Lipka V, Burton RA, Panstruga R, Strizhov N, Schulze-Lefert P, Fincher GB (2003) An *Arabidopsis* callose synthase, GSL5, is required for wound and papillary callose formation. *Plant Cell* **15**: 2503–2513
- Jacobson EL, Jacobson MK (1976) Pyridine nucleotide levels as a function of growth in normal and transformed 3T3 cells. *Arch Biochem Biophys* **175**: 627–634
- Jagtap P, Szabo C (2005) Poly(ADP-ribose) polymerase and the therapeutic effects of its inhibitors. *Nat Rev Drug Discov* **4**: 421–440
- Jambunathan N, Mahalingam R (2006) Analysis of *Arabidopsis* growth factor gene 1 (*GFG1*) encoding a nudix hydrolase during oxidative signaling. *Planta* **224**: 1–11
- Jones JD, Dangl JL (2006) The plant immune system. *Nature* **444**: 323–329
- Kim MG, da Cunha L, McFall AJ, Belkadir Y, DeRoy S, Dangl JL, Mackey D (2005) Two *Pseudomonas syringae* type III effectors inhibit RIN4-regulated basal defense in *Arabidopsis*. *Cell* **121**: 749–759
- Koh DW, Lawler AM, Poitras ME, Sasaki M, Wattler S, Nehls MC, Stoger T, Poirier GG, Dawson VL, Dawson TM (2004) Failure to degrade poly(ADP-ribose) causes increased sensitivity to cytotoxicity and early embryonic lethality. *Proc Natl Acad Sci USA* **101**: 17699–17704
- Kovalchuk I, Kovalchuk O, Kalck V, Boyko V, Filkowski J, Heinlein M, Hohn B (2003) Pathogen-induced systemic plant signal triggers DNA rearrangements. *Nature* **423**: 760–762
- Kudakasseril GJ, Minocha SC (1986) Kinetics of phenylalanine ammonia-lyase and the effect of L- α -aminoxy- β -phenylpropionic acid on enzyme activity and radicle growth in germinating lettuce seeds. *Plant Cell Physiol* **27**: 1499–1506
- Kunkel BN, Bent AF, Dahlbeck D, Innes RW, Staskawicz BJ (1993) *RPS2*, an *Arabidopsis* disease resistance locus specifying recognition of *Pseudomonas syringae* strains expressing the avirulence gene *avrRpt2*. *Plant Cell* **5**: 865–875
- Lawton MA, Lamb CJ (1987) Transcriptional activation of plant defense genes by fungal elicitor, wounding, and infection. *Mol Cell Biol* **7**: 335–341
- Lee S, Sharm Y, Lee TK, Chang M, Davis KR (2001) Lignification induced by pseudomonads harboring avirulent genes on *Arabidopsis*. *Mol Cells* **12**: 25–31
- Levine A, Tenhaken R, Dixon R, Lamb C (1994) H₂O₂ from the oxidative burst orchestrates the plant hypersensitive disease response. *Cell* **79**: 583–593
- Lucht JM, Mauch-Mani B, Steiner HY, Metraux JP, Ryals J, Hohn B (2002) Pathogen stress increases somatic recombination frequency in *Arabidopsis*. *Nat Genet* **30**: 311–314
- Masson M, Niedergang C, Schreiber V, Muller S, Menissier-de Murcia J, de Murcia G (1998) XRCC1 is specifically associated with poly(ADP-ribose) polymerase and negatively regulates its activity following DNA damage. *Mol Cell Biol* **18**: 3563–3571
- Mauch-Mani B, Slusarenko AJ (1996) Production of salicylic acid precursors is a major function of phenylalanine ammonia-lyase in the resistance of *Arabidopsis* to *Peronospora parasitica*. *Plant Cell* **8**: 203–212
- McDowell JM, Simon SA (2008) Molecular diversity at the plant-pathogen interface. *Dev Comp Immunol* **32**: 736–744
- McNellis TW, Mudgett MB, Li K, Aoyama T, Horvath D, Chua N-H, Staskawicz BJ (1998) Glucocorticoid-inducible expression of a bacterial avirulence gene in transgenic *Arabidopsis* induces hypersensitive cell death. *Plant J* **14**: 247–257
- Molinier J, Ries G, Zipfel C, Hohn B (2006) Transgenerational memory of stress in plants. *Nature* **442**: 1046–1049
- Neill S, Desikan R, Hancock J (2002) Hydrogen peroxide signalling. *Curr Opin Plant Biol* **5**: 388–395
- Newman LJ, Perazza DE, Juda L, Campbell MM (2004) Involvement of the R2R3-MYB, AtMYB61, in the ectopic lignification and dark-photomorphogenic components of the *det3* mutant phenotype. *Plant J* **37**: 239–250

- Nicholson RL, Hammerschmidt R (1992) Phenolic compounds and their role in disease resistance. *Annu Rev Phytopathol* **30**: 369–389
- Nishimura MT, Stein M, Hou BH, Vogel JP, Edwards H, Somerville SC (2003) Loss of a callose synthase results in salicylic acid-dependent disease resistance. *Science* **301**: 969–972
- O'Farrell M (1995) ADP-ribosylation reactions in plants. *Biochimie* **77**: 486–491
- Ogawa T, Ishikawa K, Harada K, Fukusaki E, Yoshimura K, Shigeoka S (2009) Overexpression of an ADP-ribose pyrophosphatase, AtNUDX2, confers enhanced tolerance to oxidative stress in Arabidopsis plants. *Plant J* **57**: 289–301
- Ogawa T, Ueda Y, Yoshimura K, Shigeoka S (2005) Comprehensive analysis of cytosolic Nudix hydrolases in *Arabidopsis thaliana*. *J Biol Chem* **280**: 25277–25283
- Olsen KM, Lea US, Slimestad R, Verheul M, Lillo C (2008) Differential expression of four Arabidopsis PAL genes: *PAL1* and *PAL2* have functional specialization in abiotic environmental-triggered flavonoid synthesis. *J Plant Physiol* **165**: 1491–1499
- Otto H, Reche PA, Bazan F, Dittmar K, Haag F, Koch-Nolte F (2005) In silico characterization of the family of PARP-like poly(ADP-ribose) transferases (pARTs). *BMC Genomics* **6**: 139
- Pan H, Wang Y, Zhang Y, Zhou T, Fang C, Nan P, Wang X, Li X, Wei Y, Chen J (2008) Phenylalanine ammonia lyase functions as a switch directly controlling the accumulation of calycosin and calycosin-7-O-beta-D-glucoside in *Astragalus membranaceus* var. *mongholicus* plants. *J Exp Bot* **59**: 3027–3037
- Panda S, Poirier GG, Kay SA (2002) *tej* defines a role for poly(ADP-ribose) in establishing period length of the Arabidopsis circadian oscillator. *Dev Cell* **3**: 51–61
- Petrucco S (2003) Sensing DNA damage by PARP-like fingers. *Nucleic Acids Res* **31**: 6689–6699
- Phillips R, Hawkins SW (1985) Characteristics of the inhibition of induced tracheary element differentiation by 3-aminobenzamide and related compounds. *J Exp Bot* **36**: 119–128
- Prats E, Martinez F, Rojas-Molina MM, Rubiales D (2007) Differential effects of phenylalanine ammonia lyase, cinnamyl alcohol dehydrogenase, and energetic metabolism inhibition on resistance of appropriate host and nonhost cereal-rust interactions. *Phytopathology* **97**: 1578–1583
- Puchta H, Swoboda P, Hohn B (1995) Induction of intrachromosomal homologous recombination in whole plants. *Plant J* **7**: 203–210
- Roldan-Arjona T, Ariza RR (2009) Repair and tolerance of oxidative DNA damage in plants. *Mutat Res* **681**: 169–179
- Rossi R, Montecucco A, Donzelli M, Denegri M, Biamonti G, Scovassi A (2002) DNA ligase I is dephosphorylated during the execution step of topoisomerase-induced apoptosis. *Cell Death Differ* **9**: 89–90
- Rosso MG, Li Y, Strizhov N, Reiss B, Dekker K, Weisshaar B (2003) An Arabidopsis thaliana T-DNA mutagenized population (GABI-Kat) for flanking sequence tag-based reverse genetics. *Plant Mol Biol* **53**: 247–259
- Saunders JA, McClure JW (1974) The suitability of a quantitative spectrophotometric assay for phenylalanine ammonia-lyase activity in barley, buckwheat, and pea seedlings. *Plant Physiol* **54**: 412–413
- Schreiber V, Dantzer F, Ame JC, de Murcia G (2006) Poly(ADP-ribose): novel functions for an old molecule. *Nat Rev Mol Cell Biol* **7**: 517–528
- Simbulan-Rosenthal CM, Rosenthal DS, Luo R, Smulson ME (1999) Poly(ADP-ribose)ylation of p53 during apoptosis in human osteosarcoma cells. *Cancer Res* **59**: 2190–2194
- Sohn KH, Lei R, Nemri A, Jones JD (2007) The downy mildew effector proteins ATR1 and ATR13 promote disease susceptibility in *Arabidopsis thaliana*. *Plant Cell* **19**: 4077–4090
- Soylu S, Brown I, Mansfield J (2005) Cellular reactions in Arabidopsis following challenge by strains of *Pseudomonas syringae*: from basal resistance to compatibility. *Physiol Mol Plant Pathol* **66**: 232–243
- Suarez-Rodriguez MC, Adams-Phillips L, Liu Y, Wang H, Su SH, Jester PJ, Zhang S, Bent AF, Krysan PJ (2007) MEKK1 is required for flg22-induced MPK4 activation in Arabidopsis plants. *Plant Physiol* **143**: 661–669
- Thomma BP, Eggermont K, Tierens KF, Broekaert WF (1999) Requirement of functional *ethylene-insensitive 2* gene for efficient resistance of Arabidopsis to infection by *Botrytis cinerea*. *Plant Physiol* **121**: 1093–1102
- Thordal-Christensen H, Zhang Z, Wei Y, Collinge DB (1997) Subcellular localization of H₂O₂ in plants: H₂O₂ accumulation in papillae and hypersensitive response during the barley-powdery mildew interaction. *Plant J* **11**: 1187–1194
- Tian R, Zhang GY, Yan CH, Dai YR (2000) Involvement of poly(ADP-ribose) polymerase and activation of caspase-3-like protease in heat shock-induced apoptosis in tobacco suspension cells. *FEBS Lett* **474**: 11–15
- Underwood W, Somerville SC (2008) Focal accumulation of defences at sites of fungal pathogen attack. *J Exp Bot* **59**: 3501–3508
- Vanderauwera S, De Block M, Van de Steene N, van de Cotte B, Metzlauff M, Van Breusegem F (2007) Silencing of poly(ADP-ribose) polymerase in plants alters abiotic stress signal transduction. *Proc Natl Acad Sci USA* **104**: 15150–15155
- Wildermuth MC, Dewdney J, Wu G, Ausubel FM (2001) Isochorismate synthase is required to synthesize salicylic acid for plant defence. *Nature* **414**: 562–565
- Wojtaszek P (1997) Oxidative burst: an early plant response to pathogen infection. *Biochem J* **322**: 681–692
- Yu IC, Parker J, Bent AF (1998) Gene-for-gene disease resistance without the hypersensitive response in *Arabidopsis dnd1* mutant. *Proc Natl Acad Sci USA* **95**: 7819–7824